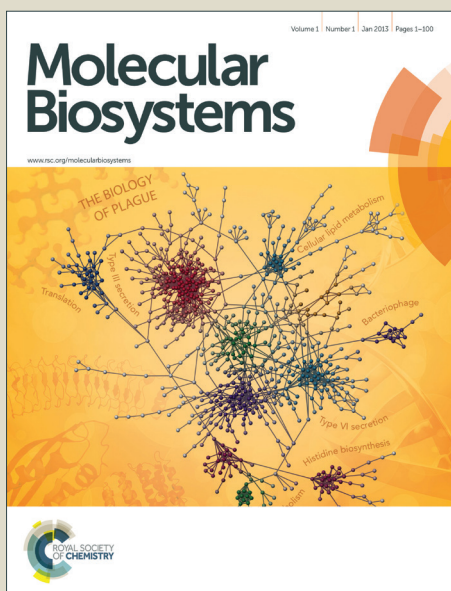


Molecular BioSystems

Accepted Manuscript



This is an *Accepted Manuscript*, which has been through the Royal Society of Chemistry peer review process and has been accepted for publication.

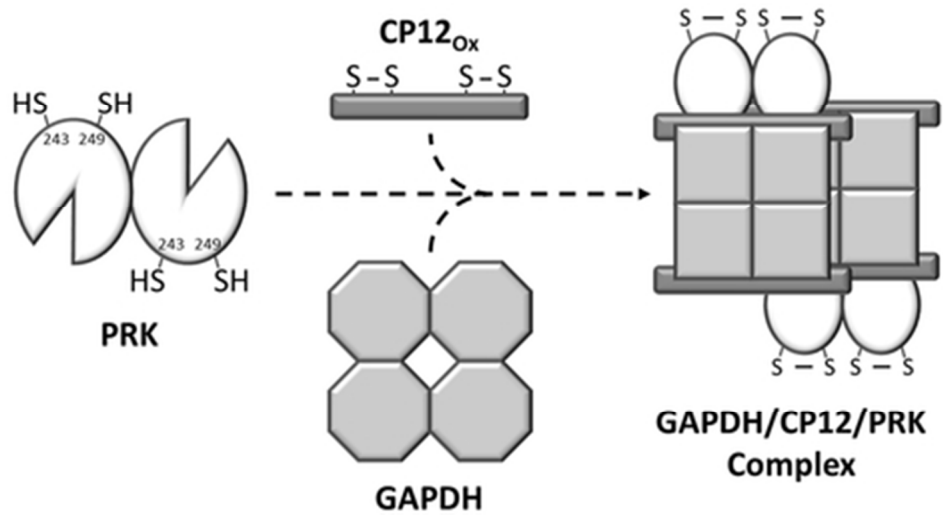
Accepted Manuscripts are published online shortly after acceptance, before technical editing, formatting and proof reading. Using this free service, authors can make their results available to the community, in citable form, before we publish the edited article. We will replace this *Accepted Manuscript* with the edited and formatted *Advance Article* as soon as it is available.

You can find more information about *Accepted Manuscripts* in the [Information for Authors](#).

Please note that technical editing may introduce minor changes to the text and/or graphics, which may alter content. The journal's standard [Terms & Conditions](#) and the [Ethical guidelines](#) still apply. In no event shall the Royal Society of Chemistry be held responsible for any errors or omissions in this *Accepted Manuscript* or any consequences arising from the use of any information it contains.



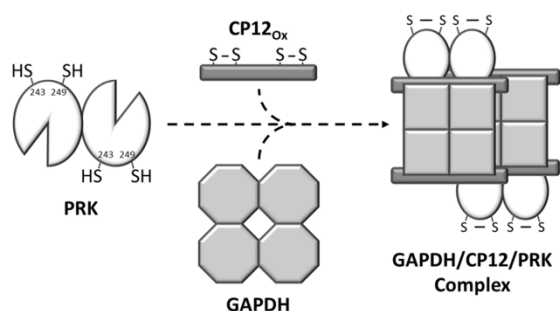
www.rsc.org/molecularbiosystems



39x21mm (300 x 300 DPI)

Phosphoribulokinase from *Chlamydomonas reinhardtii*: a Benson-Calvin Cycle enzyme enslaved to its cysteine residues.

Gabriel Thieulin-Pardo^a, Thérèse Remy^a, Sabrina Lignon^b, Régine Lebrun^b and Brigitte Gontero^{a*}



In this study, focused on *C. reinhardtii* phosphoribulokinase, we showed that CP12 catalyses a disulfide bridge between Cys243 and Cys249 on PRK. This disulfide bridge is essential for the GAPDH/CP12/PRK complex formation.

ABSTRACT

Phosphoribulokinase (PRK) in the green alga *Chlamydomonas reinhardtii* is a finely regulated and well-studied enzyme of the Benson-Calvin Cycle. PRK can form a complex with glyceraldehyde-3-phosphate dehydrogenase (GAPDH) and the small chloroplast protein CP12. This study aimed to determine the molecular determinants on PRK involved in the complex and the mechanism of action of a recently described novel regulation of PRK that involves glutathionylation. A combination of mass spectrometry, mutagenesis and activity analyses showed that Cys16, beside its role in the binding site of ATP, was the site for S-glutathionylation. Previous kinetic analysis of the C55S mutant showed that in the oxidized inactive form of PRK, this residue formed a disulfide bridge with the Cys16 residue. This is the only bridge reported for PRK in the literature. Our data show for the first time that a disulfide bridge between Cys243 and Cys249 on PRK is required to form the PRK/GAPDH/CP12 complex. These results uncover a new mechanism of the PRK/GAPDH/CP12 formation involving a thiol disulfide exchange reaction with CP12 and identify Cys16 of PRK as a target of glutathionylation acting against oxidative stress. Although Cys16 is the key residue involved in binding ATP and in defense against oxidative damage, the formation of the algal ternary complex requires the formation of another disulfide bridge on PRK involving Cys243 and Cys249.

Keywords: Glutathionylation, Intrinsically Disordered Protein, Redox regulation, CP12, Disulfide exchange, Glyceraldehyde 3-phosphate dehydrogenase, Phosphoribulokinase.

^a Aix-Marseille Université, CNRS, UMR 7281 Laboratoire de Bioénergétique et Ingénierie des Protéines, 13402 Marseille Cedex 20 France.

^b Plate-forme Protéomique, Marseille Protéomique (MaP), Institut de Microbiologie de la Méditerranée, FR 3479, CNRS, B.P. 71, 13402 Marseille Cedex 20, France.

* **Corresponding author:** Dr B. Gontero, CNRS-BIP, 31 Chemin Joseph Aiguier, 13 402 Marseille Cedex 20 France, Tel.: (+33) 491164549, Fax : (+33) 491164689, E-mail : bmeunier@imm.cnrs.fr

INTRODUCTION

Phosphoribulokinase (PRK^c, EC 2.7.1.19) is an enzyme from the Benson-Calvin Cycle that catalyzes the phosphorylation of ribulose 5-phosphate (Ru5P) into ribulose 1,5-bisphosphate (RuBP) coupled to the hydrolysis of adenosine triphosphate (ATP). The activity of the photosynthetic electron transfer chain, which produces ATP and NADPH, has a direct impact on the redox state of the chloroplast and on the activity of some of Benson-Calvin Cycle enzymes such as PRK, through the ferredoxin/thioredoxin system, among others¹. Thioredoxins are able to act directly on cysteine residues and change the redox state of their targets. PRK from higher plants and the green alga *Chlamydomonas reinhardtii* is regulated by thioredoxin^f that catalyzes the formation or disruption of a disulfide bond involving two cysteine residues of PRK (at positions 16 and 55)². The presence of this bridge inhibits the enzyme, as Cys16 belongs to the ATP binding site^{2,3} and Cys55 belongs to the active site³⁻⁵; the reduction of this disulfide bridge, in contrast, allows the enzyme to be fully activated. This mechanism is therefore reversible and, within the chloroplast, is linked to dark-light transitions. This regulation is however not present in all photosynthetic organisms: while PRKs from chlorophytes are redox regulated, PRK from other classes of photosynthetic algae (Rhodophytes, Cryptophytes and Heterokonts) display very weak or non-existent regulation via this mechanism despite the presence of both cysteine residues. The regulation has been proven to rely on the number of amino acids separating the two regulatory cysteine residues⁶. On the other hand, prokaryotic PRKs have very little in common with their eukaryote counterparts, as they lack the pair of regulatory cysteine residues and are controlled allosterically through metabolites like AMP or NADH⁷. However, the PRK isolated from the

cyanobacterium *Synechococcus sp.* PCC 7942 does possess the two regulatory cysteine residues and is redox regulated like the eukaryotic PRKs although they are separated by only 22 amino acids⁸.

Another important feature of the regulation of PRK and glyceraldehyde-3-phosphate dehydrogenase (GAPDH) is the formation of a supramolecular complex promoted by the intrinsically disordered protein, CP12⁹⁻¹⁴ (Fig. 1). Upon oxidation, CP12 forms a binary complex with GAPDH that is a fuzzy complex¹⁵; and then a ternary complex including PRK^{16,17}. Further studies allowed the identification of other partners of CP12 such as the FBP aldolase¹⁸. Embedded within the complex, the enzymes are firmly inhibited and are reactivated *in vivo*, upon reduction via the ferredoxin/thioredoxin system¹⁹⁻²¹. The GAPDH/CP12/PRK complex has been identified in the land plants *Pisum sativum*¹⁹, *Spinacia oleracea*²² and *Arabidopsis thaliana*¹³, the green alga *C. reinhardtii*²³, the red alga *Galderia sulphuraria*²⁴ and the cyanobacterium *Synechococcus* PC7942²⁵. In the freshwater diatom, *Asterionella formosa*, this ternary complex is absent and instead, a Ferredoxin-NADP reductase/GAPDH/CP12 complex has been purified; the regulation of GAPDH within this complex is consequently different from that of GAPDH interacting with PRK via CP12²⁶.

PRK and CP12 were also shown to interact in the absence of GAPDH²⁵, although their interaction is much weaker (K_d in the μM range) than the GAPDH/CP12 interaction (K_d in the nM range)¹⁰. In *C. reinhardtii*, the cysteine residues at the N-terminus of CP12 are needed for the binding of PRK, along with the middle portion of the protein²⁷. In the cyanobacterium *Synechococcus* PC7942 however, CP12 lacks the N-terminal pair of cysteine residues but is still able to interact with PRK and forms a stable and functional GAPDH/CP12/PRK complex²⁵. In both cases, little is known about which parts of the PRK protein are involved in this interaction.

Glutathione is a well-described antioxidant molecule and exists in reduced form GSH and oxidized dimeric form GSSG (linked by a disulfide bridge) in the cells²⁸⁻³². When

^c The abbreviations used are: BioGSSG: Biotin-labelled oxidized glutathione; CP12: Chloroplast Protein 12 kDa; GRX: Glutaredoxin; K_d : Dissociation constant; PRK: Phosphoribulokinase; ROS: Reactive oxygen species; Ru5P: Ribulose-5-phosphate; RuBP: Ribulose-1,5-bisphosphate; SPR: Surface plasmon resonance.

facing an oxidative stress, the cysteine residues of a protein can be irreversibly over-oxidized to sulfonic acid (-SO₃H); the glutathionylation of such a cysteine residue, *ie* the formation of a mixed disulphide with glutathione, prevents the over-oxidation of sulphhydryl groups and can be reversed by disrupting the disulphide bonds between the proteins and glutathione³¹⁻³⁴. PRK has been identified as a target of glutathionylation³⁵ and recent data showed the protective effects of glutathione on the activity of both PRK and GAPDH against oxidative stress³⁶. It seems that glutathionylation is important not only as a protection mechanism against oxidative stress, but also as a redox-related post-translational modification²⁸⁻³². As the Benson-Calvin Cycle enzymes are located within the chloroplast, they are particularly exposed to the large amounts of reactive oxygen species (ROS) resulting from photosynthesis. Their protection by glutathionylation may allow them to remain functional in this rather oxidative environment and could also prove to be a powerful mechanism to modulate the activity of the enzymes. A previous report identified two cysteine residues of PRK as potential glutathionylation targets (Cys16 and Cys243 of the *C. reinhardtii* mature protein) using crude cellular extracts³⁵. Whether the glutathionylation of PRK is a protection against over-oxidation or a post-translational regulation remains unclear.

PRK from *C. reinhardtii* has five cysteine residues (Fig. 2) and both Cys16 and Cys55 are largely conserved in the eukaryotic and cyanobacterial PRKs, although their positions, and thus the number of residues between them, may vary. The Cys61 close to the active site could have a specific role to *Chlamydomonas* PRK as it is not conserved across the eukaryotic PRK proteins. The last two cysteine residues, Cys243 and Cys249, are well conserved across the eukaryotic PRKs, with the exception of the sequences from cryptophytes, diatoms or alveolates. As each cysteine residue of the PRK from *C. reinhardtii* seems to play a role in enzyme regulation, a serine substitution mutant was generated for each of them. We chose to replace the cysteine by serine residues, as they have the most similar structure and show isosteric replacement with only a single atom

different in the side chain³⁷. These modified proteins allowed us to probe the importance of each cysteine residue in the redox regulation of PRK and the formation of the ternary GAPDH/CP12/PRK complex.

RESULTS

Determination of kinetic parameters.

A serine substitution was generated individually for each cysteine residue of *C. reinhardtii* PRK by site-directed mutagenesis; the five mutant proteins are referred to as C16S, C55S, C61S, C243S and C249S. The wild type and the mutant proteins were produced and purified following the same experimental procedure (see Experimental procedures). The activities of the mutants were measured when, either ATP was constant and ribulose-5-phosphate (Ru5P) varied or, *vice versa*. The kinetic parameters are displayed in Table 1. The catalytic constant, the K_m value and the catalytic efficiencies for the wild type are similar to those previously obtained for spinach and algal phosphoribulokinases^{5,38}. Most of the mutant proteins behave like the wild type; however, the activity of the C55S mutant was drastically affected with the catalytic constant decreased by 6 to 14 fold. The K_m values for both ATP and Ru5P increased 3 fold. The mutation of the Cys61 residue also appeared to decrease the catalytic constant of PRK by 2 fold, and the K_m values for ATP and Ru5P by about 1.5 fold. The catalytic efficiency (k_{cat} / K_m) of the C55S was decreased by 20 to 50 fold for Ru5P and ATP respectively but remains similar to that of the wild-type for all other mutants.

Evaluation of the secondary structure by circular dichroism.

To evaluate the possible structural modifications induced by the mutations, circular dichroism spectra of wild type and mutant PRKs were recorded and compared (Fig. 3). The spectra for all proteins were very similar and globally superimposed. The α helix content for the wild type PRK, based on the Equation 4, was approximately 34 % while the values calculated for the mutant proteins were very similar and

between 32 and 34%. These data indicate that there is no drastic change in the global structure of PRK upon individual cysteine substitution; however, smaller and local disruption of the protein structure could not be detected by this technique and cannot entirely be ruled out.

Identification of the glutathionylation site of PRK.

Although Cys16 and Cys243 have been identified as targets for glutathionylation³⁵, a recent study demonstrated that only one glutathione molecule was bound to each PRK monomer³⁶. To identify the glutathionylation site on purified proteins, each mutant and the wild type PRK were treated with biotinylated glutathione (BioGSSG). The samples were analyzed by Western blot (Fig. 4). Antibodies against the algal PRK showed that the amount of proteins in all samples was identical. In contrast, antibodies raised against biotin recognized the PRK band in every BioGSSG-treated sample except for the C16S one. These results indicate that the wild type PRK and each cysteine mutant, except for C16S, can be glutathionylated.

The activity of the wild type and all the mutant proteins after 2 mM GSSG treatment was then tested (Fig. 5). While the wild type and most of the mutant proteins were strongly inactivated under these conditions with only 15% to 25% of their initial activity remaining, the C16S protein was not significantly affected (remaining activity of 87%). After reduction of the GSSG-treated samples by DTT, a complete reactivation was observed for all the PRKs (83% to 106%).

The number of glutathione molecules bound to the wild type protein, the C16S and the C243S protein was measured by mass spectrometry. For these three PRKs, the spectra for the untreated samples and for the GSSG-treated samples were recorded. A fraction of the GSSG-treated proteins was subsequently reduced by DTT (Fig. 6). As previously described in the case of the wild type PRK³⁶, the mass spectrum from the untreated sample displayed a major peak at m/z 37943.6 which corresponds to the molecular mass of one PRK monomer. The GSSG-treated sample however

showed an additional peak at m/z 38249.8, which corresponded to a mass increment of 306.2 Da consistent with one glutathione molecule bound to one PRK monomer (Fig. 6A). Moreover, the addition of DTT to the GSSG-treated sample resulted in a spectrum identical to that of the PRK sample without GSSG treatment indicating an inter-disulfide bridge between the bound glutathione and PRK that is disrupted by DTT. The spectra recorded for the C16S mutant regardless the treatment with GSSG, were all similar with only one major peak at m/z 37931.6 which meant that none of the other cysteine residue than Cys16 could be glutathionylated in our conditions (Fig. 6B). In this experiment, the C243S mutant behaved exactly like the wild type protein, the spectrum recorded after GSSG treatment displays two peaks (at m/z of 37920.7 and 38226.7), which corresponds to a mass increment of 306 Da consistent with one glutathione molecule.

In order to test the influence of the glutathionylation on the binding of ATP by PRK, We performed an ATP-agarose chromatography, where ATP has been chemically bound to the gel. Pre-reduced PRK samples were treated with GSSG or not and loaded onto two identical columns. It appears that the untreated PRK sample (A), is retained on the resin and is eluted by the addition of ATP. The glutathionylated PRK is however not retained by the resin, indicating that the modification of the cysteine 16 residue by glutathione, probably through a steric hindrance effect, prevents ATP binding (Fig.7).

In our experiments, Cys16 is the only residue that could be glutathionylated on *C. reinhardtii* PRK.

Involvement of Cys243 and Cys249 in the GAPDH/CP12/PRK complex formation.

Mutant PRKs were tested for their ability to form the ternary GAPDH/CP12/PRK complex to assess the role of each cysteine in complex formation. To reconstitute this complex, a stoichiometry of 2 tetrameric GAPDH, 2 dimeric PRK and 4 monomeric CP12 (molar concentration) were used as described by Avilan *et al.* and Kaaki *et al.*^{27,39}. Native PAGE

followed by immunoblotting experiments showed that the ternary complex was formed with the wild type protein as well as with the C16S, C55S and C61S mutants (Fig. 8). However, the antibodies raised against PRK showed that free wild type and mutant PRKs (arrow 3) coexist with the complex (arrow 1). The C243S and C249S PRKs were not able to form the ternary complex, although the GAPDH/CP12 complex (arrow 2) was present. This result indicates that the Cys243 and Cys249 residues play a crucial role in the ternary complex formation, probably as a consequence of a disulfide bridge between these two residues.

PRK samples treated with reduced DTT then mixed with pre-oxidized CP12 were analyzed by mass spectrometry after a tryptic digestion (Fig. 9, Tables 2 and 3). Among the peptides identified for each sample, the oxidation state of the cysteine residues, and the presence of a Cys243-Cys249 disulfide bridge were assessed. In the presence of oxidized CP12, two ions with m/z ratios of 3395.6 and 3523.7 were observed (Table 3, Fig. 9B). These ions match the expected m/z ratios calculated for the tryptic dipeptide on PRK linked by the disulfide bridge between Cys243 and Cys249 (Fig. 9D). In contrast, when PRK was treated with DTT only and not by CP12, no disulfide bridge linking Cys243 and Cys249 could be detected for PRK (Table 2, Fig. 9C). This indicates that the formation of a disulfide bridge between the residues Cys243 and Cys249 is possible but requires the presence of oxidized CP12 as a catalyst. These results suggest a Cys243-Cys249 disulfide bridge may be essential to the GAPDH/CP12/PRK complex formation.

DISCUSSION

Phosphorylation/dephosphorylation is the best known post-translational modification, but the role of a set of versatile redox modifications of key cysteine residues is now coming to the fore. Formation of disulfide bonds is important in the structure, folding and stability of proteins^{40,41} and regulation of enzyme activity. PRK is a key enzyme of the Benson-Calvin Cycle, and its redox regulation has been intensely studied over the past years^{2,10,21,25,35,42-}

⁴⁴. Early work showed that while the oxidized form of this enzyme is inactive, the reduced form is active^{45,46}. The inactivation, upon air oxidation, was correlated, by titration of free cysteine content, to the loss of two cysteine residues as a consequence of the formation of one disulfide bridge on PRK⁴⁷. This mechanism, *in vivo*, involves small regulatory proteins, thioredoxins⁴⁵, that are able to reduce under light, or oxidize under dark, some target proteins^{1,21,48}. The activation of the spinach enzyme is initiated by nucleophilic attack by Cys46 of thioredoxin on Cys55 of PRK that exists in a disulfide bridge with Cys16 in the inactive form of the enzyme. The Cys49 on thioredoxin is then involved in the cleavage of the transient mixed disulfide formed between thioredoxin and spinach PRK⁴⁹.

Five mutants on *C. reinhardtii* PRK, C16S, C55S, C61S, C243S and C249S were generated and their kinetic parameters determined (Table 1). All the mutants, like the wild-type PRK, exhibited classical Michaelis-Menten hyperbolic kinetics with respect to both ATP and Ru5P. The kinetic parameters obtained are in agreement with the literature, and the observed effects of the mutations are similar to those reported by Brandes *et al.*⁵. For spinach PRK, Cys16 is not critical for catalysis^{3-5,50,51}, while Cys55 substitution has a significant impact on catalysis^{5,52,53}. The mutant with the greatest effect on PRK was the one lacking the Cys55 residue. The activity of the C61S mutant was also altered, but to a lesser extent, which is consistent with the proximity of Cys61 in the primary sequence to the active site and the sugar binding domain⁵⁴. All the other mutants displayed a behavior identical to the wild type protein, indicating that their direct participation in the activity of PRK is unlikely. Circular dichroism data on PRK and its mutants showed that the mutations did not introduce large changes in the secondary structure of the proteins. Moreover, the spectra indicate that PRK is composed of both α helix and β sheet, in agreement with the modeling of *C. reinhardtii* PRK (Fig. 2) with a α helix content of about 34 %.

Beside the redox regulatory system, described above, the reducing power delivered

from the electron transport in the primary phase of photosynthesis, is also distributed to an antioxidant system. Reduction of soluble antioxidant such as glutathione is used to defend cell components against reactive oxygen species²⁸⁻³². Again, cysteine residues are at the heart of this mechanism. Previous studies have shown that GSSG has a strong reversible inhibitory power over PRK^{35,36}. This phenomenon can be reversed by reduction which is performed by the glutaredoxins (GRXs) *in vivo*^{31-33,35}. Glutathionylation of PRK is impeded by the presence of its substrates, Ru5P and ATP, which indicates that the glutathionylation occurs near or at the active site³⁶. Mass spectrometry has confirmed that only one cysteine residue is glutathionylated on each PRK monomer³⁶, while two glutathionylation sites were previously identified: Cys16 and Cys243³⁵. Using biotinylated glutathione labeling, activity measurements and mass spectrometry, the Cys16 residue was shown to be the only glutathionylable site of the algal PRK *in vitro*, while Cys243 glutathionylation was never observed in our experiments. This result is not surprising since this residue is highly reactive, involved in the redox-regulated disulfide bridge (Cys16-Cys55), and in the ATP-binding site of the protein^{3,4}. The involvement of the Cys16 residue is further confirmed by the inability of the glutathionylated protein to bind ATP, as the bulk of a glutathione molecule in the middle of the ATP-binding site would prevent the nucleotide to dock through a steric hindrance effect. The modification by glutathionylation of Cys16 on PRK is however not a typical protection mechanism of cysteine residues from irreversible oxidation to sulfinic (-SO₂H) or sulfonic (-SO₃H) acids as Cys16 is not essential to the catalytic process, but can be seen more as a post-translational modification as it was described in other key regulatory enzymes^{35,55-58}. Glutathionylation can also constitute a mode of regulation, as it can modulate the activity of target enzymes and thereby play a role in many cellular processes³⁴.

Lastly, there is considerable evidence that PRK interacts with GAPDH and CP12, leading to the formation of a ternary complex^{10,13,14,17,22,27}, however, the only residue

on PRK known to impede the complex formation is the Arg64 residue (see Fig. 2)¹⁶. Two of the PRK mutants, C243S and C249S, were unable to form the GAPDH/CP12/PRK complex, pointing out the involvement of Cys243 and Cys249 in this process. These two residues are relatively well conserved across photosynthetic organisms (Fig. 10); and are always conserved as a pair; none of the sequences contains only one of them. However, some PRKs lack the Cys243-Cys249 couple altogether and these PRKs belong to organisms from which the GAPDH/CP12/PRK complex has never been identified, such as the freshwater diatom *A. formosa*²⁶ and other diatoms^{59,60}. Moreover, a modeled structure of a PRK monomer (Fig. 2) shows that Cys243 and Cys249 should be in close proximity, which may allow for the formation of a disulfide link. These data suggest that the Cys243-Cys249 couple is a molecular determinant for the GAPDH/CP12/PRK complex formation and thereby the regulation of PRK and GAPDH.

The modeling of the PRK structure (based on the PRK monomer from *Rhodobacter sphaeroides*⁶¹) allows us to speculate that Cys243 and Cys249 are very close and could therefore easily form a disulfide bridge. Mass spectrometry experiments showed that in presence of oxidized CP12, a Cys243-Cys249 disulfide bridge (Fig. 9) was identified on PRK, suggesting that CP12 was able to trigger its formation. Based on the observations reported here, we propose that the Cys243-Cys249 disulfide bridge formation might be catalyzed by oxidized CP12 in a thiol-disulfide exchange mechanism similar to the one previously reported with CP12 and GAPDH⁴⁵. The requirement for oxidized CP12 as a catalyst to form this bridge could explain why it has not been identified in the past^{2,3,5,27,38,43}. Moreover, this region is well conserved among PRK sequences, and also is flanked by proline residues, known to be crucial residues for protein-protein interactions⁶². The Cys243-Cys249 bridge on PRK would therefore be required for the stable association of PRK with its partners.

To conclude, PRK is clearly under the influence of multiple redox regulation

mechanisms, probably triggered by different circumstances and acting on different timescales.

EXPERIMENTAL

PRK mutagenesis.

Site-directed mutagenesis of the cysteine residues was performed by PCR on the expression vector pET28a where the PRK coding sequence had previously been inserted²⁷. The mutagenesis reactions were carried out using the kit Quickchange II (Agilent Technologies, Santa Clara, California) according to the manufacturer's instructions. The primers were synthesized by Eurofins Genomics (Luxembourg). After the reaction, PCR products were transformed into *E. coli* competent cells Rosetta (DE3) pLysS (Merck Millipore, Billerica, Massachusetts). After colony PCR screening, the plasmids from positive clones, were purified with the Wizard Plus minipreps kit (Promega, Fitchburg, Wisconsin) and the presence of each mutation was verified by sequencing (GATC Biotech AG, Konstanz, Germany).

Recombinant proteins production and purification.

The mutant PRK proteins were produced and purified using the same method used to obtain the recombinant wild type protein²⁷. Recombinant CP12 and GAPDH proteins were also produced and purified as previously described^{10,63}.

Protein concentration measurements.

Protein concentrations were estimated using the Bradford method with BSA as a standard⁶⁴.

PRK activity assays.

PRK activity assays are based on the Racker method⁶⁵ by coupling the ATP dephosphorylation catalyzed by PRK to the oxidation of NADH via pyruvate kinase and lactate dehydrogenase¹⁶ NADH disappearance at

340 nm was followed with a Lambda 25 spectrophotometer (Perkin-Elmer, Waltham, Massachusetts) at 25°C.

Determination of kinetic parameters.

Michaelis constants (K_m) and catalytic constants (k_{cat}) of the wild type and mutant PRKs were determined experimentally from activity measurements with either ATP constant (1 mM) and varying Ru5P concentrations (1-1000 μ M) and *vice versa*. Wild type and mutant PRK concentrations in the samples were between 10 and 70 nM. The observed velocities were reported as a function of the substrate concentration and the resulting data were fitted to the Michaelis equation (Equation 1):

$$V = \frac{V_{max} \times [S]}{K_m + [S]}$$

where, V is the enzymatic activity (U), V_{max} the maximal enzymatic activity (U), $[S]$ the substrate concentration (μ M), and K_m the Michaelis constant (μ M). The catalytic constant k_{cat} was determined from Equation 2:

$$k_{cat} = \frac{V_{max}}{E_0}$$

where, E_0 is the enzyme concentration (in M).

Circular dichroism.

Proteins were diluted in filtered 50 mM Na_2HPO_4 pH7 and placed in a 2 mm quartz cuvette; final protein concentration was around 1 μ M. Spectra were recorded from 260 to 185 nm on a Jasco J-1100 spectropolarimeter (Jasco Analytical Instruments, Easton, Maryland) at 25°C. Each spectrum was the result of 8 successive scans. In order to allow comparison between proteins, raw ellipticity E (mdeg) was converted into mean residue molar ellipticity θ ($\text{deg} \cdot \text{cm}^2 \cdot \text{dmol}^{-1}$) using Equation 3:

$$\theta = \frac{E \times 10^6}{l \times C \times N}$$

where, l is the pathlength of the cuvette (mm), C is the protein concentration of the sample (μ M) and N is the number of peptide bonds of the protein (for PRK, $N = 338$). The α helix content

(τ_α in percentage) of the wild type and mutant proteins was calculated using Equation 4⁶⁶:

$$\tau_\alpha = \frac{100 \cdot \theta_{222} \times N}{39500 \times (2.57 - N)}$$

where θ_{222} is the mean residue molar ellipticity θ (deg.cm².dmol⁻¹) measured at 222 nm.

BioGSSG assays.

A biotinylated tag (EZ-link sulphy-NHS biotin (Thermo Scientific, Waltham, Massachusetts)) was chemically added to oxidized glutathione molecules to detect glutathionylation using Western blotting, as previously described³⁵. Biotinylated glutathione is hereafter noted BioGSSG. Proteins were incubated with 2 mM BioGSSG for 1 h at room temperature before being treated with 100 mM iodoacetamide (IAM) and 20 mM *N*-ethylmaleimide (NEM). Samples were separated by SDS-PAGE electrophoresis performed according to the Laemmli method⁶⁷ using 12% gels. After migration, proteins were stained using Coomassie blue or blotted onto a nitrocellulose membrane. After protein transfer, membranes were stained with Red Ponceau, blocked with milk powder and then incubated 1 h at room temperature in the presence of primary rabbit antibodies raised against biotin or PRK diluted 10,000 fold. After thorough washing, the membranes were incubated for 1 h at room temperature in the presence of a 1:10,000 dilution of secondary donkey antibodies raised against rabbit IgG (GE Healthcare, Little Chalfont, United Kingdom) conjugated with the horseradish peroxidase. The blots were then revealed by standard chemiluminescence techniques.

Effect of GSSG on PRK activity.

The activity of wild type and mutant PRKs samples was measured as described above after they were treated with 2 mM GSSG for 30 min at room temperature or kept untreated. The activity of GSSG-treated samples was measured again after they were subsequently reduced using 20 mM DTT for an additional

20 min. For each sample, measurements were expressed as percentage of the untreated activity.

ATP-agarose affinity chromatography.

Reduced PRK samples were treated or not with 2 mM GSSG for 1 h at room temperature. 5 μ g of each sample were loaded onto ATP-agarose resin (Sigma-Aldrich, St Louis, Missouri, USA) equilibrated with 10 mM phosphate buffer pH 7.5 supplemented with 0.1 mM EDTA (height and diameter of the column were 2 cm and 0.7 cm respectively, and the flow rate was 0.7 mL.min⁻¹). After incubation with the resin for 1h, and after washing, bound proteins were eluted by 1 mM ATP. The proteins were monitored by absorbance measurements at 280 nm, while the PRK activity was measured as described above after reduction by 20 mM DTT for 20 min.

Mass spectrometry.

Global mass analysis. Wild type and mutant PRK were analyzed by MALDI-ToF mass spectrometry (Microflex II, Bruker Daltonics, Billerica, Massachusetts) after 30 min incubation at 25°C in the presence or the absence of 2 mM GSSG. A fraction of each GSSG-treated sample was also reduced using 20 mM DTT for 30 min at room temperature prior to MALDI-ToF mass spectrometry analysis. 10 to 20 pmol of each protein samples were spotted onto a MALDI stainless steel target plate and mixed with an equal volume of a saturated solution of matrix sinapinic acid (40% CH₃CN in water, 0.1% Trifluoroacetic acid (v/v)). Mixtures were dried at room temperature. Acquisition of spectra was performed on a Microflex II mass spectrometer (Bruker Daltonics, Billerica, Massachusetts) in linear and positive mode with a pulsed ion extraction, using the Flex control software and applying external calibration by the Protein calibration Standard I (Bruker Daltonics, Billerica, Massachusetts).

Identification of disulfide bridges. Wild type PRK samples were incubated at room temperature for 20 min with 20 mM reduced

DTT. After desalting on a Nick column (GE Healthcare Little Chalfont, United Kingdom), part of the reduced sample was mixed with pre-oxidized CP12 in a 2:1 CP12:PRK ratio and kept at room temperature for 30 min (CP12 was oxidized by incubation with 5 mM CuCl₂ for 20 min, excess Cu²⁺ was removed by Nick column). The final PRK concentration in all samples was 0.1 μM. Reduced cysteine residues were blocked by treatment with 1.8 μM iodoacetamide for 30 min at room temperature in the dark, then samples were digested overnight at 37 °C in presence of 312 nM of trypsin (Promega, Fitchburg, Wisconsin). After acidification by a solution of 12,5 % TFA in water, the samples were firstly desalting on Zip Tip C18 units according to the manufacturer's protocol (Millipore, Darmstadt, Deutschland), then spotted onto a MALDI stainless steel target plate, together with an equal volume of a saturated solution of matrix alpha cyano-4-hydroxycinnamic acid (70% CH₃CN in water 0.1% trifluoacetic acid (v/v)). The mixtures were left to dry at room temperature. Acquisition of spectra was performed on the same MALDI-ToF mass spectrometer as described above, but in positive reflectron mode and applying external calibration by the Peptide Calibration Standard (Bruker Daltonics, Billerica, Massachusetts). A peak list generated by the PMF_PS method on the FlexAnalysis software was manually checked and an internal calibration with the theoretical values of tryptic peptides from PRK was applied. Data were then processed with the Biotools software using the following parameters: optional modification of cysteine (disulfide bridges (-2 Da), carbamidomethyl (+57 Da)), oxidation of methionine (+16 Da), 4 missed cleavages and a mass tolerance ±30 ppm.

GAPDH/CP12/PRK complex reconstitution.

Wild type and each mutant PRK (0.09 nmol), GAPDH (0.09 nmol) and CP12 (0.18 nmol) were mixed and incubated 14 h at 4°C in 30 mM Tris-HCl, pH 7.9, 4 mM EDTA, 0.1 mM NAD and 5 mM cysteine in a final volume of 50 μl. In some experiments cysteine was replaced by oxidized DTT. The formation of the PRK-GAPDH-CP12 complex was visualized

by native PAGE performed using the PhastSystem and precast gradient 4-15 % gels (PhastGel, GE Healthcare, Little Chalfont, United Kingdom) as previously described²⁷. After migration, proteins were stained using Coomassie blue and/or blotted onto a nitrocellulose membrane to be revealed by immunoblot. After protein transfer, membranes were stained with Red Ponceau, blocked with low fat milk powder and then incubated 1 h at room temperature in the presence of primary rabbit antibodies raised against PRK, CP12 or GAPDH diluted 10,000 times. After extensive washing, the membranes were incubated for 1 h at room temperature in the presence of a 1:10,000 dilution of secondary donkey antibodies raised against rabbit IgG (GE Healthcare, Little Chalfont, United Kingdom) conjugated with the horseradish peroxidase. The blots were then revealed by standard chemiluminescence technique.

Multiple alignments of PRK sequences.

PRK sequences were obtained from the NCBI Protein Database (<http://www.ncbi.nlm.nih.gov/genbank>): *Arabidopsis thaliana* (#NP_174486.1), *Spinacia oleracea* (#CAA30499.1), *Chlorella variabilis* (#EFN55598.1), *Galdieria sulphuraria* (#CAC80070.1), *Cyanidioschyzon merolae* (#XP_005535773.1), *Chondrus crispus* (#XP_005716677.1), *Euglena gracilis* (#AAX13964.1), *Emiliania huxleyi* (#XP_005767208.1), *Isochrysis galdana* (#AAW79322.1), *Prymnesium parvum* (#AAX13966.1), *Guillardia theta* (#XP_005827680.1), *Vaucheria litorea* (#AFA52561.1), *Heterosigma akashiwo* (#ABQ42600.1), *Odontella sinensis* (#CAA69902.2), *Thalassiosira pseudonana* (#EED92818.1), *Phaeodactylum tricorutum* (#ACI65926.1), *Heterocapsa triquetra* (#AAW79321.1), *Lingulodinium polyedrum* (#AAX13961.1), *Bigelowiella natans* (#AAP79209.1), *Synechococcus elongatus* (#YP_171277.1), *Thermosynechococcus elongatus* (#YP_171277.1). Sequences were aligned using Clustalw (<http://www.clustal.org>),

and the alignment was treated by Genedoc (<http://www.nrbcs.org/gfx/genedoc>).

CONCLUSION

In this study, we identified Cys16 as the major glutathionylation site of the *C. reinhardtii* protein and unveiled the involvement of Cys243 and Cys249, whose functions remained unidentified, in the GAPDH/CP12/PRK complex formation. During this process, oxidized CP12 can catalyze a disulfide/thiol exchange and form the Cys243-Cys249 bridge on PRK, which is mandatory for the ternary complex formation.

ACKNOWLEDGMENTS

Fellowship (Gabriel Thieulin-Pardo) was given by Ecole Normale Supérieure, Cachan. This work (BG) was supported by the Centre National de la Recherche Scientifique (CNRS) and Aix-Marseille Université, La Région PACA, APO project 063 506.

We thank Dr Michael E. Salvucci for the kind gift of PRK antiserum.

REFERENCES

1. P. Schurmann and J. P. Jacquot, *Annu. Rev. Plant Physiol. Plant Mol. Biol.*, 2000, 51, 371-400.
2. M. A. Porter, C. D. Stringer and F. C. Hartman, *J. Biol. Chem.*, 1988, 263, 123-129.
3. J. Omnaas, M. A. Porter and F. C. Hartman, *Arch. Biochem. Biophys.*, 1985, 236, 646-653.
4. H. K. Brandes, C. D. Stringer and F. C. Hartman, *Biochemistry*, 1992, 31, 12833-12838.
5. H. K. Brandes, F. C. Hartman, T. Y. Lu and F. W. Larimer, *J. Biol. Chem.*, 1996, 271, 6490-6496.
6. S. C. Maberly, C. Courcelle, R. Groben and B. Gontero, *J. Exp. Bot.*, 2010, 61, 735-745.
7. H. M. Miziorko, in *Adv. Enzymol. Relat. Areas Mol. Biol.*, John Wiley & Sons, Inc., 2006, pp. 95-127.
8. D. Kobayashi, M. Tamoi, T. Iwaki, S. Shigeoka and A. Wadano, *Plant Cell Physiol.*, 2003, 44, 269-276.
9. B. Gontero and S. C. Maberly, *Biochem. Soc. Trans.*, 2012, 40, 995-999.
10. E. Graciet, P. Gans, N. Wedel, S. Lebreton, J. M. Camadro and B. Gontero, *Biochemistry*, 2003, 42, 8163-8170.
11. R. Groben, D. Kaloudas, C. A. Raines, B. Offmann, S. C. Maberly and B. Gontero, *Photosynth. Res.*, 2010, 103, 183-194.
12. P. E. Lopez-Calcagno, T. P. Howard and C. A. Raines, *Front. Plant. Sci.*, 2014, 5, 9.
13. L. Marri, P. Trost, P. Pupillo and F. Sparla, *Plant Physiol.*, 2005, 139, 1433-1443.
14. L. Marri, P. Trost, X. Trivelli, L. Gonnelli, P. Pupillo and F. Sparla, *J. Biol. Chem.*, 2008, 283, 1831-1838.
15. E. Mileo, M. Lorenzi, J. Eroles, S. Lignon, C. Puppo, N. Le Breton, E. Etienne, S. R. Marque, B. Guigliarelli, B. Gontero and V. Belle, *Mol. Biosyst.*, 2013, 9, 2869-2876.
16. L. Avilan, B. Gontero, S. Lebreton and J. Ricard, *Eur. J. Biochem.*, 1997, 250, 296-302.
17. L. Avilan, B. Gontero, S. Lebreton and J. Ricard, *Eur. J. Biochem.*, 1997, 246, 78-84.
18. J. Eroles, L. Avilan, S. Lebreton and B. Gontero, *FEBS J.*, 2008, 275, 1248-1259.
19. T. P. Howard, M. Metodiev, J. C. Lloyd and C. A. Raines, *Proc. Natl. Acad. Sci. U. S. A.*, 2008, 105, 4056-4061.
20. S. Lebreton, B. Gontero, L. Avilan and J. Ricard, *Eur. J. Biochem.*, 1997, 246, 85-91.
21. L. Marri, M. Zaffagnini, V. Collin, E. Issakidis-Bourguet, S. D. Lemaire, P. Pupillo, F. Sparla, M. Miginiac-Maslow and P. Trost, *Mol. Plant*, 2009, 2, 259-269.
22. S. Clasper, J. S. Easterby and R. Powls, *Eur. J. Biochem.*, 1991, 202, 1239-1246.
23. S. Lebreton, E. Graciet and B. Gontero, *J. Biol. Chem.*, 2003, 278, 12078-12084.
24. C. Oesterheld, S. Klocke, S. Holtgreffe, V. Linke, A. P. Weber and R. Scheibe, *Plant Cell Physiol.*, 2007, 48, 1359-1373.
25. M. Tamoi, T. Miyazaki, T. Fukamizo and S. Shigeoka, *Plant J.*, 2005, 42, 504-513.
26. M. Mekhalfi, C. Puppo, L. Avilan, R. Lebrun, P. Mansuelle, S. C. Maberly and B. Gontero, *New Phytol.*, 2014, 203, 414-423.
27. L. Avilan, C. Puppo, J. Eroles, M. Woudstra, R. Lebrun and B. Gontero, *Mol. Biosyst.*, 2012, 8, 2994-3002.
28. H. Z. Chae, H. Oubrahim, J. W. Park, S. G. Rhee and P. B. Chock, *Antioxid. Redox. Signal.*, 2012, 16, 506-523.
29. P. Ghezzi, V. Bonetto and M. Fratelli, *Antioxid. Redox. Signal.*, 2005, 7, 964-972.

30. J. J. Mięyal and P. B. Chock, *Antioxid. Redox. Signal.*, 2012, 16, 471-475.
31. G. Noctor, A. Mhamdi, S. Chaouch, Y. Han, J. Neukermans, B. Marquez-Garcia, G. Queval and C. H. Foyer, *Plant Cell Environ.*, 2012, 35, 454-484.
32. M. Zaffagnini, M. Bedhomme, S. D. Lemaire and P. Trost, *Plant Sci.*, 2012, 185-186, 86-96.
33. C. H. Foyer and G. Noctor, *Plant Physiol.*, 2011, 155, 2-18.
34. M. Zaffagnini, M. Bedhomme, C. H. Marchand, S. Morisse, P. Trost and S. D. Lemaire, *Antioxid. Redox. Signal.*, 2012, 16, 567-586.
35. M. Zaffagnini, M. Bedhomme, H. Groni, C. H. Marchand, C. Puppo, B. Gontero, C. Cassier-Chauvat, P. Decottignies and S. D. Lemaire, *Mol. Cell. Proteomics.*, 2012, 11, M111 014142.
36. L. Marri, G. Thieulin-Pardo, R. Lebrun, R. Puppo, M. Zaffagnini, P. Trost, B. Gontero and F. Sparla, *Biochimie*, 2014, 97, 228-237.
37. T. E. Creighton, in *Proteins: Structures and Molecular Properties*, W. H. Freeman and Co, New York, 1983, ch. 1, pp. 1-60.
38. L. Avilan, S. Lebreton and B. Gontero, *J. Biol. Chem.*, 2000, 275, 9447-9451.
39. W. Kaaki, M. Woudstra, B. Gontero and F. Halgand, *Rapid Commun Mass Spectrom*, 2013, 27, 179-186.
40. T. E. Creighton, *Biol. Chem.*, 1997, 378, 731-744.
41. K. L. Peña, S. E. Castel, C. de Araujo, G. S. Espie and M. S. Kimber, *Proc. Nat. Ac. Sci. U. S. A.*, 2010, 107, 2455-2460.
42. F. Mouche, B. Gontero, I. Callebaut, J. P. Mornon and N. Boisset, *J. Biol. Chem.*, 2002, 277, 6743-6749.
43. M. K. Geck and F. C. Hartman, *J. Biol. Chem.*, 2000, 275, 18034-18039.
44. M. Hirasawa, P. Schurmann, J. P. Jacquot, W. Manieri, P. Jacquot, E. Keryer, F. C. Hartman and D. B. Knaff, *Biochemistry*, 1999, 38, 5200-5205.
45. B. B. Buchanan, *Annu. Rev. Plant Physiol.*, 1980, 31, 341-374.
46. R. A. Wolosiuk and B. B. Buchanan, *Arch. Biochem. Biophys.*, 1978, 189, 97-101.
47. M. A. Porter, S. Milanez, C. D. Stringer and F. C. Hartman, *Arch. Biochem. Biophys.*, 1986, 245, 14-23.
48. M. Balsera, E. Uberegui, P. Schurmann and B. B. Buchanan, *Antioxid. Redox. Signal.*, 2014.
49. H. K. Brandes, F. W. Larimer and F. C. Hartman, *J. Biol. Chem.*, 1996, 271, 3333-3335.
50. T. J. Krieger, L. Mende-Mueller and H. M. Mizioro, *Biochim. Biophys. Acta*, 1987, 915, 112-119.
51. T. J. Krieger and H. M. Mizioro, *Biochemistry*, 1986, 25, 3496-3501.
52. S. Milanez, R. J. Mural and F. C. Hartman, *J. Biol. Chem.*, 1991, 266, 10694-10699.
53. M. A. Porter and F. C. Hartman, *J. Biol. Chem.*, 1988, 263, 14846-14849.
54. M. G. Sandbaken, J. A. Runquist, J. T. Barbieri and H. M. Mizioro, *Biochemistry*, 1992, 31, 3715-3719.
55. M. Bedhomme, M. Adamo, C. H. Marchand, J. Couturier, N. Rouhier, S. D. Lemaire, M. Zaffagnini and P. Trost, *Biochem. J.*, 2012, 445, 337-347.
56. M. Bedhomme, M. Zaffagnini, C. H. Marchand, X. H. Gao, M. Moslonka-Lefebvre, L. Michelet, P. Decottignies and S. D. Lemaire, *J. Biol. Chem.*, 2009, 284, 36282-36291.
57. G. Kim and R. L. Levine, *Antioxid. Redox. Signal.*, 2005, 7, 849-854.
58. M. Zaffagnini, L. Michelet, C. Marchand, F. Sparla, P. Decottignies, P. Le Marechal, M. Miginiac-Maslow, G. Noctor, P. Trost and S. D. Lemaire, *FEBS J.*, 2007, 274, 212-226.
59. A. K. Michels, N. Wedel and P. G. Kroth, *Plant Physiol.*, 2005, 137, 911-920.
60. C. Wilhelm, C. Buchel, J. Fisahn, R. Goss, T. Jakob, J. Laroche, J. Lavaud, M. Lohr, U. Riebesell, K. Stehfest, K. Valentin and P. G. Kroth, *Protist*, 2006, 157, 91-124.
61. D. H. Harrison, J. A. Runquist, A. Holub and H. M. Mizioro, *Biochemistry*, 1998, 37, 5074-5085.
62. R. M. Kini and H. J. Evans, *Biochem. Biophys. Res. Commun.*, 1995, 212, 1115-1124.
63. E. Graciet, S. Lebreton, J. M. Camadro and B. Gontero, *Eur. J. Biochem.*, 2003, 270, 129-136.
64. M. M. Bradford, *Anal. Biochem.*, 1976, 72, 248-254.
65. E. Racker, *Arch. Biochem. Biophys.*, 1957, 69, 300-310.
66. Y. H. Chen, J. T. Yang and K. H. Chau, *Biochemistry*, 1974, 13, 3350-3359.
67. U. K. Laemmli, *Nature*, 1970, 227, 680-685.

FIGURE LEGENDS

Figure 1: Schematic view of the GAPDH/CP12/PRK complex formation. GAPDH (tetrameric form) binds two CP12 proteins, causing a conformational change to occur that allows the dimeric form of phosphoribulokinase (PRK) to bind as well. This GAPDH/CP12/PRK unit then dimerizes to give the fully-formed supramolecular GAPDH/CP12/PRK complex.

Figure 2: Modeled structure of the phosphoribulokinase from *C. reinhardtii*. Swiss-Model (<http://swissmodel.expasy.org/>) was used to make a model of the PRK monomer from *C. reinhardtii* (NCBI Accession #EDP02974.1) based on the structure of the PRK monomer from *Rhodobacter sphaeroides* (PDB code 1a7j.1.A)⁶¹. Cysteine residues are represented by black spheres and the arginine residue Arg64 by grey spheres.

Figure 3: Circular dichroism spectra from wild type and mutant phosphoribulokinases. Spectra were recorded from 180 to 260 nm; 8 successive spectra were accumulated for each protein. The proteins were used at a final concentration of 1 μ M in filtered 50 mM NaH₂PO₄, pH 7. The spectrum of the wild type PRK is displayed in solid lines, while the spectra of the mutant proteins are shown in dotted lines for C16S, in short dashes for C55S, in dashes and double dots for C61S, in long dashes for C243S and in dashes and simple dots for C249S.

Figure 4: Glutathionylation of wild type and mutant PRKs followed by Western blot. The wild type and mutant proteins were incubated in the presence or the absence of 2 mM BioGSSG before 1 μ g of proteins was loaded on 12.5 % SDS-PAGE. After migration, proteins were stained using Coomassie blue (top panel) or blotted onto a nitrocellulose membrane to be revealed by western blot using antibodies raised against Biotin (middle panel) or PRK (bottom panel) diluted 10,000 times. The lane noted L corresponds to the molecular weight ladder (Prestained Protein Ladder, Euromedex).

Figure 5: Effect of GSSG on the PRK wild type, C16S and C243S activity. The activity of wild type and mutant PRKs was measured after treatment with 2 mM GSSG for 30 min at room temperature (white bars) or kept untreated (black bars). The activity of GSSG-treated samples was measured again after reduction using 20 mM DTT for 20 additional min (white dashed bars). For each protein, the untreated sample was used as standard. (not significant (ns): $p > 0.1$; *: $p < 0.05$; **: $p < 0.01$; ***: $p < 0.001$; $n = 4$).

Figure 6: Glutathionylation of wild type, C16S and C243S PRKs analyzed by mass spectrometry. Wild type (A), C16S (B) and C243S (C) PRKs were analyzed by MALDI-ToF in linear and positive mode. In every panel, the untreated samples are shown in solid lines, samples incubated for 30 min with 2 mM GSSG in long dashes and samples treated with GSSG and subsequently incubated with 20 mM DTT for 20 additional min in dotted lines. m/z Ratios are highlighted for the most intense peaks. A systematic additional peak following the major peak was observed in all our experiments, corresponding to a matrix sinapinic acid adduct of 203 Da.

Figure 7: Comparison of elution profiles of the untreated and glutathionylated PRKs on ATP-agarose columns. Reduced wild type PRK (A) or reduced and treated with 2 mM GSSG (B) were loaded

onto ATP-agarose columns. The proteins were subsequently eluted by addition of 1 mM ATP (arrows). The proteins were monitored by measuring the absorbance at 280 nm and the PRK activity measured after 20 mM DTT reduction as described in Experimental section.

Figure 8: *In vitro* reconstitution of the GAPDH/CP12/PRK complex for the wild type and mutant PRKs. Wild type or mutant PRKs (0.09 nmol), GAPDH (0.09 nmol) and CP12 (0.18 nmol) were incubated 12 h at 4°C in 30 mM Tris, 4mM EDTA, 0.1 mM NAD and 5 mM cysteine, pH7.9. The samples were separated on 4-15 % native PAGEs (PhastGel, GE Healthcare) and proteins were subsequently revealed using Coomassie staining or immunoblots anti-PRK, anti-CP12 and anti-GAPDH antibodies. From top to bottom, the arrows indicate: the GAPDH/CP12/PRK complex (arrow 1), the GAPDH/CP12 complex (arrow 2), free GAPDH and PRK (arrow 3) and free CP12 (arrow 4).

Figure 9: Identification of the Cys243-Cys249 disulfide bridge by mass spectrometry. A pre-reduced sample of wild type PRK was incubated with pre-oxidized CP12. The final PRK concentration in all the samples was 0.1 μM. Free cysteine residues were blocked by treatment with 1.8 μM iodoacetamide, samples were digested by trypsin. (A) Entire spectrum. The m/z of the most intense peaks deriving from PRK and CP12 are respectively underlined or indicated by an asterisk. The complete list of the peptides identified is available in Table 3. (B) and (C) Close-up on the 3500-3550 region of the PRK + CP12_{ox} (B) and PRK_{red} (C) spectra containing the peak corresponding to the peptides linked by the Cys243-Cys249 disulfide (D).

Figure 10: Multiple alignment of PRK sequences in the Cys243-Cys249 region of the *C. reinhardtii* protein. Black, dark grey and light grey indicate respectively 80% or above, 70% and 60% identities. The positions of the Cys243 and Cys249 residues of the *C. reinhardtii* protein are indicated by arrows. The sequences were obtained from the NCBI Protein Database (<http://www.ncbi.nlm.nih.gov/genbank>) (See experimental procedures for the detailed list) and aligned using Clustalw (<http://www.clustal.org>), the alignment was treated by Genedoc (<http://www.nrbcs.org/gfx/genedoc>).

TABLES

Table 1: Experimentally determined K_m and k_{cat} of the wild type and mutant PRKs. Michaelis constants (K_m) and catalytic constants (k_{cat}) were determined from activity measurements in presence of a range in ATP or Ru5P concentrations (1-1000 μ M), while the other substrate was kept constant at 1 mM. The comparison between each value and its equivalent for the wild type protein is displayed in the *Rel. WT* columns as the ratio between mutant and WT parameters (K_m , k_{cat}).

| | | K_m (μ M) | <i>Rel. WT</i> | k_{cat} (s^{-1} .site $^{-1}$) | <i>Rel. WT</i> |
|------|-------|------------------|----------------|--------------------------------------|----------------|
| ATP | WT | 33.8 \pm 6.0 | 1 | 235 \pm 11 | 1 |
| | C16S | 31.2 \pm 1.4 | 0.92 | 274 \pm 2.7 | 1.2 |
| | C55S | 114 \pm 0.9 | 3.4 | 16.8 \pm 0.5 | 0.071 |
| | C61S | 21.8 \pm 1.1 | 0.64 | 116 \pm 1.3 | 0.49 |
| | C243S | 30.2 \pm 1.4 | 0.89 | 239 \pm 2.7 | 1.0 |
| | C249S | 37.4 \pm 2.2 | 1.1 | 236 \pm 2.9 | 1.0 |
| Ru5P | WT | 87.5 \pm 5.2 | 1 | 262 \pm 4.3 | 1 |
| | C16S | 87.6 \pm 5.4 | 1.0 | 275 \pm 4.7 | 1.0 |
| | C55S | 271 \pm 19 | 3.1 | 46.8 \pm 3.6 | 0.18 |
| | C61S | 63.1 \pm 2.1 | 0.72 | 169 \pm 1.4 | 0.65 |
| | C243S | 80.4 \pm 2.3 | 0.92 | 269 \pm 4.1 | 1.0 |
| | C249S | 86.7 \pm 7.1 | 0.99 | 270 \pm 6.4 | 1.0 |

Table 2: Experimental peak list obtained for reduced PRK after trypsin digestion. PRK was reduced using 20 mM DTT. Free cysteine residues were blocked by treatment with 1.8 μ M iodoacetamide prior to trypsin digestion. The identified peptides cover 68.4 % of the PRK sequence.

| No | Measured m/z | Theoretical m/z | Range | Sequence and modifications |
|----|--------------|-----------------|-----------|--|
| 1 | 1150.684 | 1150.629 | 246 - 255 | KLTCSEFPGIK |
| 2 | 1194.662 | 1194.625 | 143 - 152 | IYLDISDDIK |
| 3 | 1278.619 | 1278.618 | 6 - 18 | MVIGLAADSGCGK (Carbamidomethyl (C)) |
| 4 | 1357.678 | 1357.682 | 297 - 307 | FYGEITQQMLK |
| 5 | 1436.689 | 1436.706 | 179 - 190 | KPDFDAYIDPQK |
| 6 | 1436.689 | 1436.706 | 180 - 191 | PDFDAYIDPQKK |
| 7 | 1932.94 | 1932.898 | 6 - 23 | MVIGLAADSGCGKSTFMR (2 Oxidation (M), Carbamidomethyl (C)) |
| 8 | 1932.94 | 1932.991 | 280 - 296 | LEELIYVESHLNNTSAK |
| 9 | 2082.03 | 2082.087 | 97 - 115 | SVDKPIYNHVSGLIDAPEK |
| 10 | 2124.146 | 2124.149 | 143 - 159 | IYLDISDDIKFAWKIQR |
| 11 | 2209.082 | 2209.096 | 71 - 90 | GVTALAPEAQNFDMYNQVK |
| 12 | 2223.156 | 2223.217 | 116 - 134 | IESPPILVIEGLHPFYDKR |
| 13 | 2266.129 | 2266.233 | 134 - 152 | RVAELLDKFIYLDISDDIK |
| 14 | 2433.152 | 2433.125 | 225 - 245 | MFDPVYLFDEGSTISWIPCGR |
| 15 | 2490.221 | 2490.147 | 225 - 245 | MFDPVYLFDEGSTISWIPCGR (Carbamidomethyl (C)) |
| 16 | 2506.129 | 2506.142 | 225 - 245 | MFDPVYLFDEGSTISWIPCGR (Oxidation (M), Carbamidomethyl (C)) |
| 17 | 2858.367 | 2858.232 | 256 - 280 | MFYGPDTWYGQEVSVLEMDGQFDK (Oxidation (M)) |
| 18 | 2899.499 | 2899.535 | 192 - 216 | DADMIIQVLPTQLVPDDKGGQYLRVR (Oxidation (M)) |
| 19 | 3065.64 | 3065.504 | 6 - 34 | MVIGLAADSGCGKSTFMRRMTSIFGGVPK (3 Oxidation (M)) |

Table 3: Experimental peak list obtained for PRK incubated with oxidized CP12 after trypsin digestion. A pre-reduced sample of wild type PRK was incubated with pre-oxidized CP12. Free cysteine residues were blocked by treatment with 1.8 μ M iodoacetamide prior to trypsin digestion. Peptides belonging to the CP12 protein are highlighted in grey; peptides containing the Cys243-Cys249 disulfide bridge are displayed in bold. The identified peptides cover 52 % and 80 % of the PRK and CP12 sequences respectively.

| No | Measured m/z | Theoretical m/z | Range | Sequence and modifications |
|----|-----------------|-----------------|------------------|--|
| 1 | 836.392 | 836.345 | 39 - 46 | EAEDACAK |
| 2 | 965.541 | 965.512 | 246 - 255 | LTCSFPGIK |
| 3 | 1093.646 | 1093.607 | 246 - 255 | KLTCFPGIK |
| 4 | 1194.671 | 1194.625 | 143 - 152 | IYLDISDDIK |
| 5 | 1278.644 | 1278.618 | 6 - 18 | MVIGLAADSGCGK (Carbamidomethyl (C)) |
| 6 | 1296.673 | 1296.636 | 20 - 31 | HMSGQPAVDLTK |
| 7 | 1357.7 | 1357.682 | 297 - 307 | FYGEITQQMLK |
| 8 | 1424.721 | 1424.731 | 20 - 32 | HMSGQPAVDLNKK |
| 9 | 1522.762 | 1522.746 | 75 - 88 | ADVTLTDPLEAFCK |
| 10 | 1564.794 | 1564.801 | 181 - 191 | KPDFDAYIDPQKK |
| 11 | 1579.813 | 1579.767 | 75 - 88 | ADVTLTDPLEAFCK (Carbamidomethyl (C)) |
| 12 | 1932.959 | 1932.898 | 6 - 23 | MVIGLAADSGCGKSTFMR (2 Oxidations (M), Carbamidomethyl (C)) |
| 13 | 1932.959 | 1932.991 | 280 - 296 | LEELIYVESHLNNTSAK |
| 14 | 2209.003 | 2209.096 | 71 - 90 | GVTALAPEAQNFDMYNQVK |
| 15 | 2346.947 | 2347.087 | 47 - 69 | GTSADCAVAWDTVEELSAVSHK |
| 16 | 2404.006 | 2404.109 | 47 - 69 | GTSADCAVAWDTVEELSAVSHK (Carbamidomethyl (C)) |
| 17 | 2490.061 | 2490.147 | 225 - 245 | MFDPVYLFDEGSTISWPCGR |
| 18 | 2628.261 | 2628.37 | 192 - 214 | DADMIIQVLPTQLVPDDKGYLR |
| 19 | 2842.147 | 2842.237 | 251 - 274 | MFYGPDTWYGQEVSVLEMDGQFDK |
| 20 | 2955.199 | 2955.43 | 20 - 46 | HMSGQPAVDLNKKVQDAVKEAEDACAK (Oxidation (M)) |
| 21 | 2999.26 | 2999.292 | 75 - 101 | ADVTLTDPLEAFCKDAPDADECRVYED (Disulfide (SS)) |
| 22 | 3162.37 | 3162.399 | 39 - 69 | EAEDACAKGTSADCAVAWDTVEELSAVSHK (Disulfide (SS)) |
| 23 | 3395.593 | 3395.615 | 225 - 245 | MFDPVYLFDEGSTISWPCGR (Disulfide bridge with [LTCSFPGIK]) |
| 24 | 3412.583 | 3412.52 | 71 - 101 | DAVKADVTLTDPLEAFCKDAPDADECRVYED (Disulfide (SS)) |
| 25 | 3523.72 | 3523.71 | 225 - 246 | MFDPVYLFDEGSTISWPCGRK (Disulfide bridge with [LTCSFPGIK]) |
| 26 | 4249.296 | 4249.14 | 210 - 245 | GQYLRVRLIMKEGSKMFDPVYLFDEGSTISWPCGR |

Figure 1

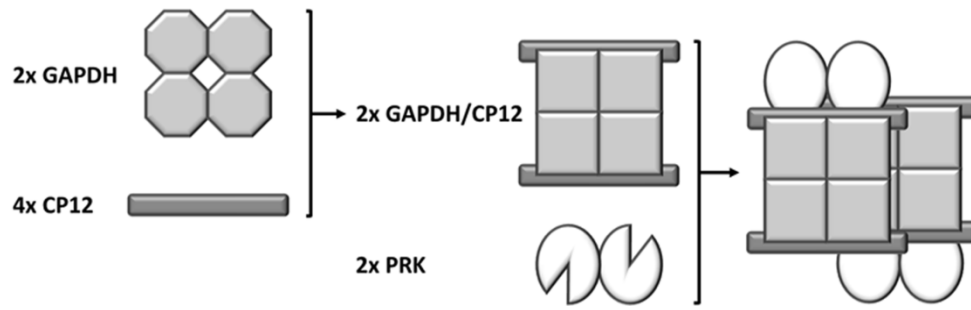


Figure 2

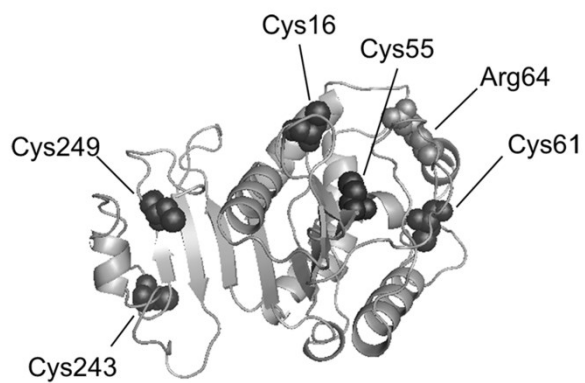


Figure 3

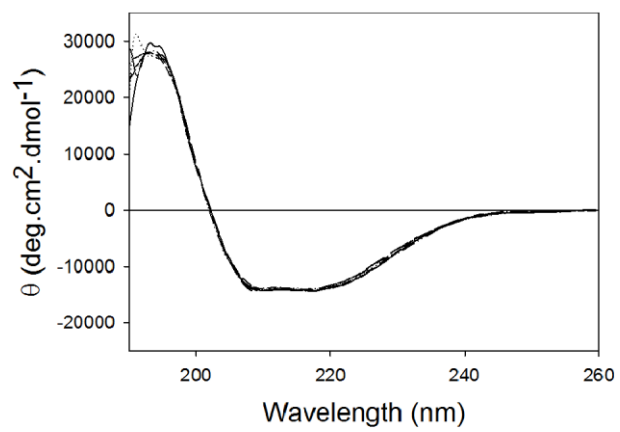


Figure 4

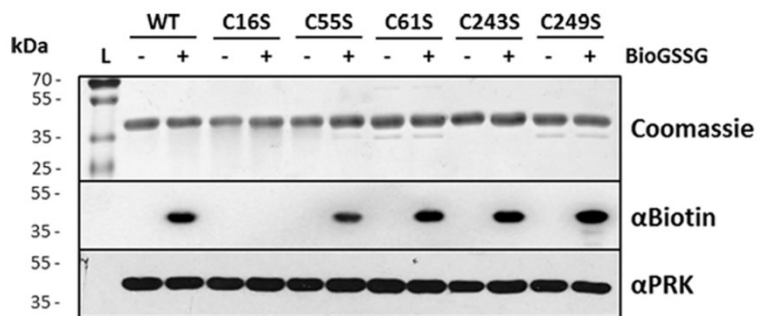


Figure 5

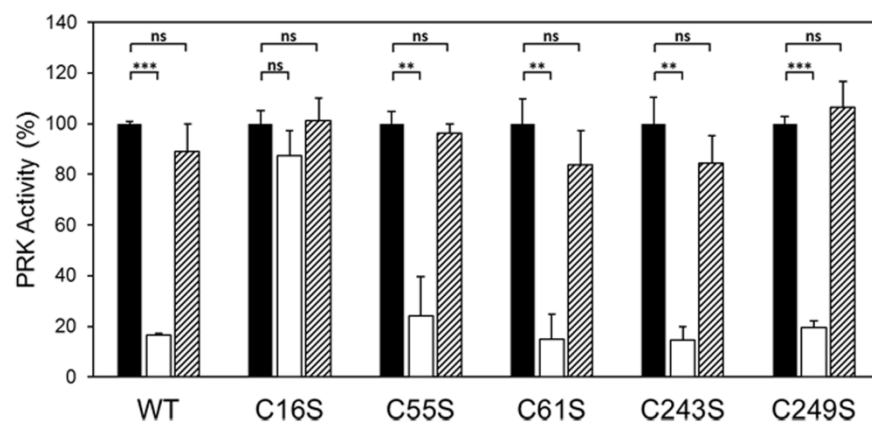


Figure 6

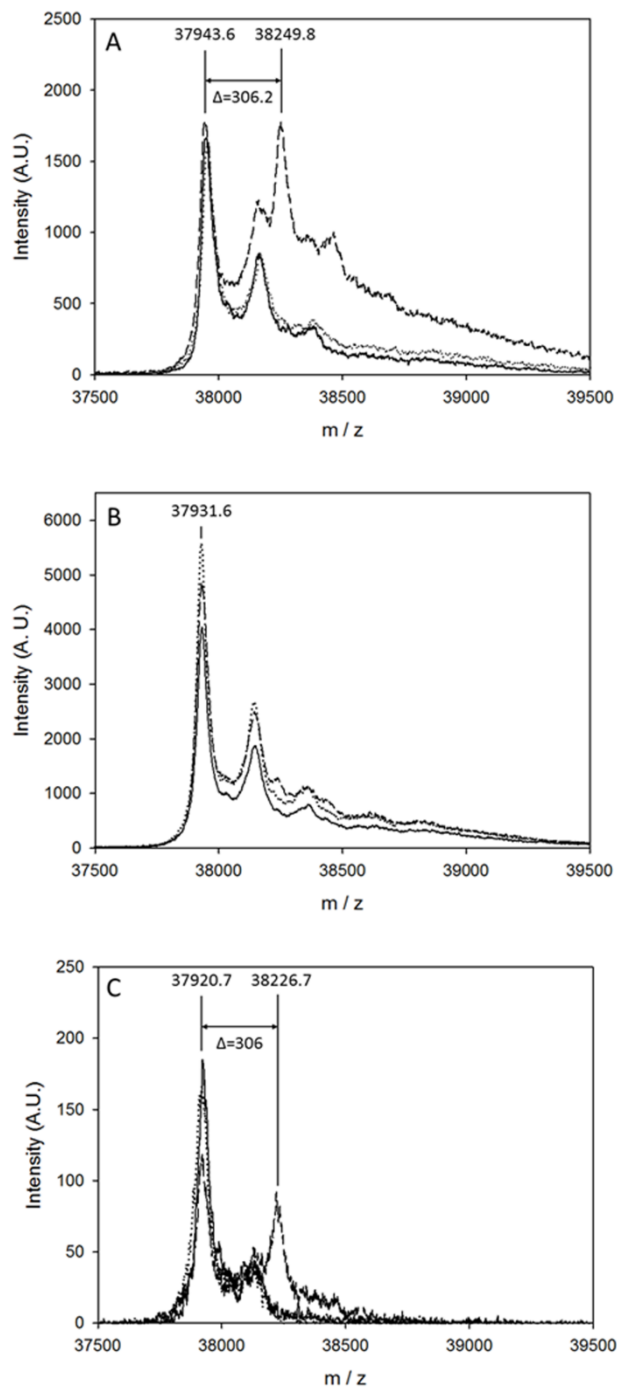


Figure 7

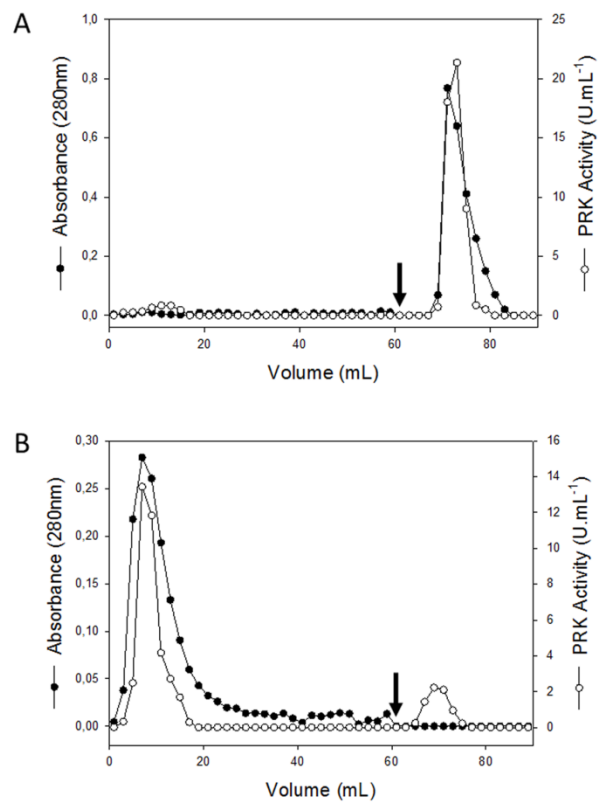


Figure 8

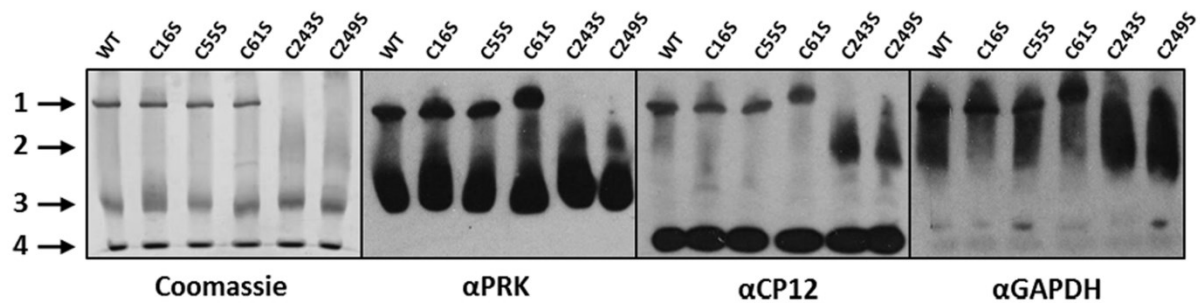


Figure 9

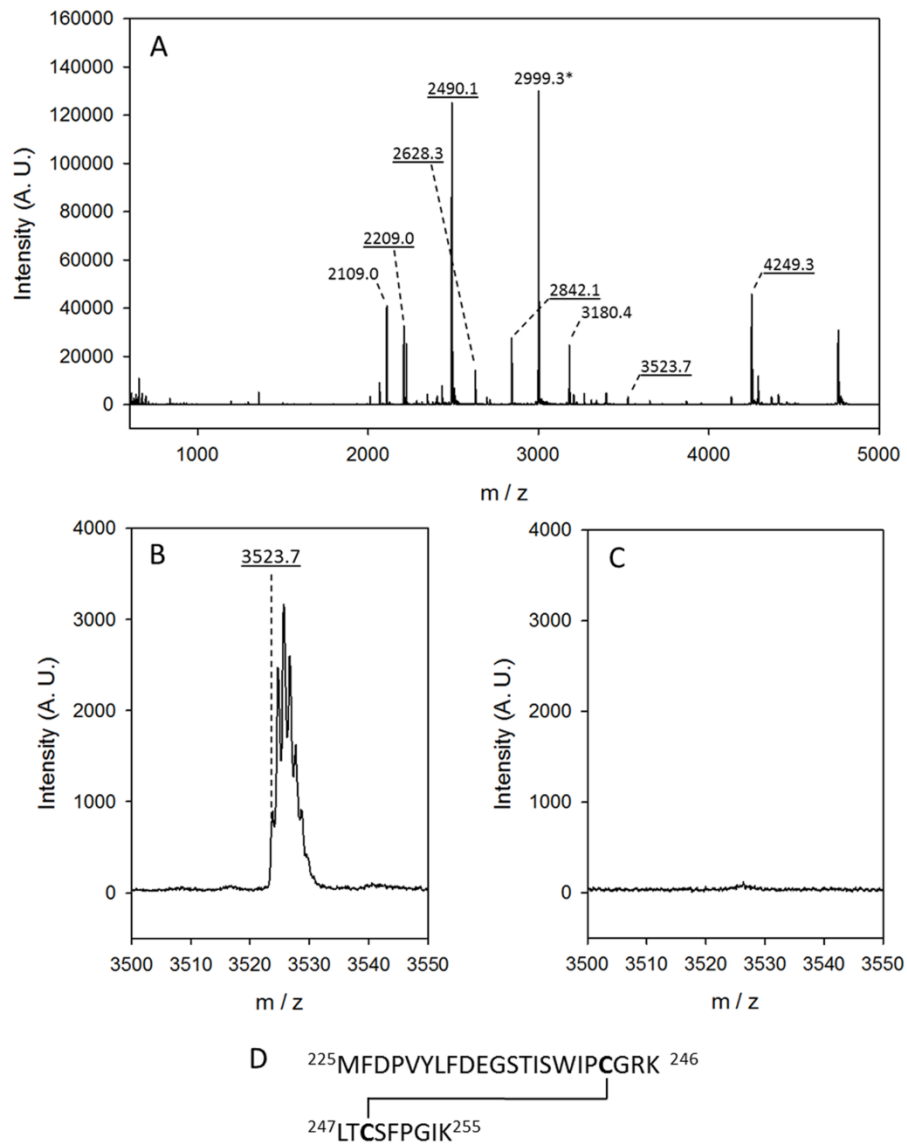


Figure 10

C. reinhardtii 187 : DPQRKADMI IQVLEPTQIV-PDD-KG---KVLRVRLIMREGSKM DPVYLFD-EGSTLSWIEPCGR--KLTCSPGII--KMFYGPDTWYGQEVSVLEMD : 274
 A. thaliana 187 : DPQRQYADWIEVLEPTQII-PDDNEG---KVLRVRLIMREGVKYS SPVYLFD-EGSTLSWIEPCGR--KLTCSPGII--KFNVEPDSYHDHEVSVLEMD : 275
 S. oleracea 187 : DPQRQHADVIEVLEPTQII-PDDDEG---KVLRVRLIMREGVKFN PVYLFD-EGSTLSWIEPCGR--KLTCSPGII--KFSYGPDTYMGNEVTVVLEMD : 275
 Chlorella sp. 187 : DPQRKADMI IQVLEPTQIV-PDETEK---KVLRVRLIMREGKLL DPVYLFD-QGSTLSWIEPCGR--KLTCSPGII--KMFYGPDTYMGQEVSVLEMD : 275
 G. sulphuraria 180 : DPQRKADVAVIQVLEPTQII-PDDETEK---KVLRVRLIMREGIQGQSQSVYLFD-EGSTLSWIEPCGR--KLTCSPGII--KFHYGPDNWNHDSVLEMD : 268
 C. merolae 180 : DPQRQYADWIEVLEPTQII-PEDKER---KVLRVRLIMREGVQGS KTAFLFD-EGSTLSWIEPCGR--KLTCSPGII--KFHYGPESFYGADFSSTLEMD : 268
 C. crispus 180 : DPQRKADVAVIQVLEPTQII-PDDETEK---KVLRVRLIMREGVQGS KTAFLFD-EGSTLSWIEPCGR--KLTCSPGII--KFHYGPDNWNHDSVLEMD : 268
 E. gracilis 192 : APQRKADWIEVLEPTQII-PPKDETAPELVRVRIQR TTTKH DPVYLFD-KGSSVTKPCGD--NLCQEPGII--QLAYYTEEMGHFPAVLEMD : 283
 E. huxleyi 191 : BPQRKADWIEVLEPTQII-E-DPTG---KVLKVKVLRQKSKVTC AETPVYLD-EGSTLSWIEPCGR--KLTCSPGII--VLSYDDEWEGEAVSVLEMD : 278
 I. galbana 191 : BPQRKADWIEVLEPTQII-D-DATG---KVLKVKVLRQKSKVTC AETPVYLD-EGSTLSWIEPCGR--KLTCSPGII--VLSYDDEWEGEAVSVLEMD : 278
 P. parvum 191 : BPQRKADWIEVLEPTQII-D-DPTG---KVLKVKVLRQKSKVTC AETPVYLD-EGSTLSWIEPCGR--KLTCSPGII--VLSYDDEWEGEAVSVLEMD : 278
 G. theta 186 : DPQRKADWIEVLEPTQII-V-A--NDK---THLVKVLQCKGV DHAETPVYLD-EGSTLSWIEPCGR--KLTCSPGII--KFRYGTETMVGSEVTVLEMD : 274
 P. lutheri 186 : APQRANADWIEVLEPTQII-V-N-DAEG---KVLKVKVLRQKSKVTC AETPVYLD-EGSTLSWIEPCGR--KLTCSPGII--KFRYGTETMVGSEVTVLEMD : 273
 V. litorea 192 : APQRKADWIEVLEPTQII-V-PEDKEG---KVLKVKVLRQKSKVTC AETPVYLD-EGSTLSWIEPCGR--KLTCSPGII--KFRYGTETMVGSEVTVLEMD : 280
 H. akashiwo 192 : SPQRKADWIEVLEPTQII-PDSTDG---KVLKVKVLRQKSKVTC AETPVYLD-EGSTLSWIEPCGR--KLTCSPGII--KFRYGTETMVGSEVTVLEMD : 280
 O. sinensis 192 : APQRKADWIEVLEPTQII-E--EDK---KVLKVKVLRQKSKVTC AETPVYLD-EGSTLSWIEPCGR--KLTCSPGII--KFRYGTETMVGSEVTVLEMD : 278
 T. pseudonana 192 : BPQRKADWIEVLEPTQII-D-K--EDK---KVLKVKVLRQKSKVTC AETPVYLD-EGSTLSWIEPCGR--KLTCSPGII--KFRYGTETMVGSEVTVLEMD : 278
 P. tricornutum 182 : DPQRKADWIEVLEPTQII-D-Q--DDK---KVLKVKVLRQKSKVTC AETPVYLD-EGSTLSWIEPCGR--KLTCSPGII--KFRYGTETMVGSEVTVLEMD : 278
 H. triquetra 180 : DPQRKADWIEVLEPTQII-V--DKGL---PVLKVKVLRQKSKVTC AETPVYLD-EGSTLSWIEPCGR--KLTCSPGII--KFRYGTETMVGSEVTVLEMD : 252
 L. polyedrum 180 : DPQRKADWIEVLEPTQII-V--DKGL---PVLKVKVLRQKSKVTC AETPVYLD-EGSTLSWIEPCGR--KLTCSPGII--KFRYGTETMVGSEVTVLEMD : 252
 B. natans 180 : BPQRANADWIEVLEPTQII-V-DVAPGEET---KVLKVKVLRQKSKVTC AETPVYLD-EGSTLSWIEPCGR--KLTCSPGII--KFRYGTETMVGSEVTVLEMD : 272
 S. elongatus 170 : BPQRGHADWIEVLEPTQII-V-PNTER---KVLKVKVLRQKSKVTC AETPVYLD-EGSTLSWIEPCGR--KLTCSPGII--KFRYGTETMVGSEVTVLEMD : 258
 T. elongatus 170 : DPQRKADWIEVLEPTQII-V-A-KEEKVVG---NVLKVKVLRQKSKVTC AETPVYLD-EGSTLSWIEPCGR--KLTCSPGII--KFRYGTETMVGSEVTVLEMD : 258